Perhalophenyl(tetrahydrothiophene)gold(I) Complexes as Lewis Bases in Acid−Base Reactions with Silver Trifluoroacetate†

Eduardo J. Fernández,*,§ Peter G. Jones,# Antonio Laguna,*,‡ José M. López-de-Luzuriaga,§ Miguel Monge,§ M. Elena Olmos,§ and Raquel C. Puelles§

Departamento de Química, Universidad de la Rioja, Grupo de Síntesis Química de La Rioja, UA-CSIC, Complejo Científico Tecnológico, 26006 Logroño, Spain, Departamento de Química Inorgánica, Instituto de Ciencia de Materiales de Aragón, Universidad de Zaragoza-CSIC, 50009 Zaragoza, Spain, and Institut für Anorganische und Analytische Chemie der Technischen Universität, Postfach 3329, D-38023 Braunschweig, Germany

Received July 13, 2007

Reaction of $[Ag(CF_3CO_2)]$ with $[Au(C_6X_5)(tht)]$ (X = halogen, tht = tetrahydrothiophene) leads to the synthesis of complexes $[AgAu(C_6F_5)(CF_3CO_2)(tht)]_n$ (**1**), $[Ag_2Au(C_6Cl_2F_3)(CF_3CO_2)_2(tht)]_n$ (**2**), or $[AgAu(C_6Cl_5)(CF_3CO_2)(tht)]_n$ (**3**), confirming the capability of a neutral complex, such as a perhalophenyl(tetrahydrothiophene)gold(I), to act as electron density donor when treated with a Lewis acid substrate. All three crystal structures have been established by X-ray diffraction; all display Au···Ag and Ag···Ag interactions and polymeric 1D (**2**, **3**) or 2D (**1**) networks built by means of additional Au···Au, Ag−O···Ag, or Au−S···Ag interactions. Complexes **1**−**3** are luminescent in the solid state at room temperature, and at 77 K or in frozen solutions they show a different luminescence in the solid state, which seems to be related to the different number and types of metal−metal interactions present in each case. DFT and TDDFT calculations on simplified model systems of **1**−**3** have also been carried out.

Introduction

Aurophilic Au(I)···Au(I) interactions have traditionally been the most studied nonbonding contacts between closed-shell metals,[1] but complexes with metallophilic interactions between gold(I) and other closed-shell metal atoms (Au···M) have attracted great interest over the past years because of their theoretical interest,[2] the photophysical properties of the complexes,[3] or their potential applications.[4] A number of species displaying Au(I)···Ag(I) interactions have been described to date, most of them containing bidentate ligands between Au^I and Ag^I,[5] although there are also compounds in which such interactions are supported only by an ylide,[5j,k] a phenylacetylide,[6] or an aryl bridging ligand[7] or even a number of examples that display unsupported Au···Ag interactions.[8] In the last few years the acid−base strategy has been shown to be an effective method for the synthesis of heteropolynuclear compounds with unsupported Au···M contacts; a number of Au^I/Tl^I or Au^I/Ag^I species displaying such interactions have been prepared by reaction of $NBu_4[Au(C_6X_5)_2]$ (X = halogen) with thallium(I)[4b,9] or silver(I)[7e,f] salts in the presence or absence of ancillary ligands, which demonstrates the capability of bis(perhalophenyl)aurate(I) anions to act as Lewis bases.

The neutral derivatives $[Au(C_6X_5)(tht)]$ (X = halogen, tht = tetrahydrothiophene) are well-known starting materials for the synthesis of gold(I) complexes through displacement reactions of the weakly coordinated ligand tht by other neutral or anionic ligands, resulting in the formation of mononuclear $[Au(C_6X_5)L]$ or $[Au(C_6X_5)X']^-$ (L, X′ = monodentate ligands) or polynuclear $[\{Au(C_6X_5)\}_nL]$ or $[\{Au(C_6X_5)\}_nX']^{n-}$ (L, X′ = polydentate ligands) compounds that often display aurophilic interactions.[10] Moreover, the pentafluorophenyl derivative $[Au(C_6F_5)(tht)]$ can also act as a deprotonating agent when it is treated with $Ph_2P(O)H$, affording the synthesis of $[H(Ph_2PO)_2Au]_2$ with displacement of tht and formation of C_6F_5H.[11] Another perhalophenyl gold(I) complex, $[Au(3,5\text{-}C_6Cl_2F_3)(tht)]$, has been found to be a very efficient catalyst for the isomerization of *trans*-$[Pd(3,5\text{-}C_6Cl_2F_3)_2(tht)_2]$ to *cis*-$[Pd(3,5\text{-}C_6Cl_2F_3)_2(tht)_2]$, in a reaction that

† Dedicated to Prof. Maria Pilar Garcia on the occasion of her 60th birthday.

* Authors to whom correspondence should be addressed. E-mail: alaguna@unizar.es; eduardo.fernandez@unirioja.es.

§ Universidad de la Rioja.

‡ Universidad de Zaragoza-CSIC.

Technische Universität Braunschweig.

(1) (a) *Gold: Progress in Chemistry, Biochemistry and Technology*; Schmidbaur, H., Ed.; John Wiley & Sons, Inc.: New York, 1999. (b) Schmidbaur, H. *Nature* **2001**, *413*, 31. (c) Schmidbaur, H. *Gold Bull.* **1990**, *23*, 11.

(2) Pyykkö, P. *Chem. Rev.* **1997**, *97*, 597.

(3) Forward, J. M.; Fackler, J. P., Jr.; Assefa, Z. In *Optoelectronic Properties of Inorganic Compounds*; Roundhill, D. M., Fackler, J. P., Jr., Eds.: Plenum: New York, 1999; pp 195−226.

(4) (a) Fernández, E. J.; Laguna, A.; López-de-Luzuriaga, J. M.; Monge, M. Spanish Patent P200001391, 2003. (b) Fernández, E. J.; López-de-Luzuriaga, J. M.; Monge, M.; Olmos, M. E.; Pérez, J.; Laguna, A.; Mohammed, A. A.; Fackler, J. P., Jr. *J. Am. Chem. Soc.* **2003**, *125*, 2022.

(5) (a) Römbke, P.; Schier, A.; Schmidbaur, H.; Cronje, S.; Raubenheimer, H. *Inorg. Chim. Acta* **2004**, *357*, 235. (b) Fernández, E. J.; López-de-Luzuriaga, J. M.; Monge, M.; Rodríguez, M. A.; Crespo, O.; Gimeno, M. C.; Laguna, A.; Jones, P. G. *Chem. Eur. J.* **2000**, *6*, 636. (c) Wang, Q.-M.; Lee, Y.-A.; Crespo, O.; Deaton, J.; Tang, C.; Gysling, H. J.; Gimeno, M. C.; Larraz, C.; Villacampa, M. D.; Laguna, A.; Eisenberg, R. *J. Am. Chem. Soc.* **2004**, *126*, 9488. (d) Olmos, M. E.; Schier, A.; Schmidbaur, H. *Z. Naturforsch.* **1997**, *52b*, 203. (e) Crespo, O.; Fernández, E. J.; Gil, M.; Gimeno, M. C.; Jones, P. G.; Laguna, A.; López-de-Luzuriaga, J. M.; Olmos, M. E. *J. Chem. Soc., Dalton Trans.* **2002**, 1319. (f) Catalano, V. J.; Horner, S. J. *Inorg. Chem.* **2003**, *42*, 8430. (g) Catalano, V. J.; Malwitz, M. A.; Etogo, A. O. *Inorg. Chem.* **2004**, *43*, 5714. (h) Catalano, V. J.; Etogo, A. O. *J. Organomet. Chem.* **2006**, *690*, 6041. (i) Rawashdeh-Omary, M. A.; Omary, M. A.; Fackler, Jr., J. P. *Inorg. Chim. Acta* **2002**, *334*, 376. (j) Vicente, J.; Chicote, M. T.; Lagunas, M. C.; Jones, P. G. *J. Chem. Soc., Chem. Commun.* **1991**, 1730. (k) Vicente, J.; Chicote, M. T.; Lagunas, M. C. *Inorg. Chem.* **1993**, *32*, 3748.

(6) (a) Abu-Salah, O. M.; Knobler, C. B. *J. Organomet. Chem.* **1986**, *302*, C10. (b) Haque, M. U.; Horne, W.; Abu-Salah, O. M. *J. Crystallogr. Spectrosc. Res.* **1992**, *2*, 421. (c) Hussain, M. S.; Haque, M. U.; Abu-Salah, O. M. *J. Clusters Sci.* **1996**, *7*, 167.

10.1021/om700701m CCC: $37.00
Publication on Web 10/24/2007

takes place through a novel reversible aryl exchange between Pd(II) and Au(I).[12] Thus, $[Au(C_6X_5)(tht)]$ have been mainly employed in displacement reactions, but their behavior as Lewis bases, similarly to $[Au(C_6X_5)_2]^-$ anions, has not been reported to date.

Considering all these precedents, we wondered if the neutral derivatives $[Au(C_6X_5)(tht)]$ could act as electron density donors when treated with a Lewis acid, such as a silver(I) salt. We therefore treated various $[Au(C_6X_5)(tht)]$ complexes with silver trifluoroacetate, which has been previously employed in acid−base reactions with the neutral complex mesitylgold(I),[7e] in order to obtain heterometallic Au^I/Ag^I systems with Au···Ag interactions. In principle, the products could display a different Au/Ag ratio depending on the halogen atoms present in the gold precursor. The crystal structures of the resulting complexes have been determined by X-ray diffraction methods, and their optical properties have been experimentally and theoretically studied in order to rationalize the results.

Results and Discussion

Synthesis and Characterization. As mentioned in the Introduction, we tried to study the influence of the perhalophenyl groups in the resulting Au/Ag complexes in order to rationalize their basic character. As expected, the gold(I) derivatives $[Au(C_6X_5)(tht)]$ (C_6X_5 = C_6F_5, 3,5-$C_6Cl_2F_3$, C_6Cl_5) react with $[Ag(CF_3CO_2)]$ in a dissimilar manner, leading to products with different stoichiometry depending on the aryl group present in the starting material (see Scheme 1).

Treatment of $[Au(C_6F_5)(tht)]$ with equimolecular amounts of $[Ag(CF_3CO_2)]$ in diethyl ether leads to the synthesis of a complex of stoichiometry $[AgAu(C_6F_5)(CF_3CO_2)(tht)]_n$ (**1**), according to the molar ratio employed, confirming that the neutral arylgold(I) derivative is also able to act as electron density donor toward the acid silver(I) salt. The same product is also obtained when the reaction is carried out in different molar ratios, such as 1:2 or 1:4, which indicates that the Au/Ag ratio depends on the perhalophenyl group and not on the molar ratio employed in the reaction. It is isolated as an air-stable white solid, whose analytical and spectroscopic data agree with the proposed formulation and that is nonconducting in acetone solution. Its IR spectrum shows, among others, absorptions at 1504 (vs), 981 (vs), and 796 (vs) cm^{-1} arising from the presence of a pentafluorophenyl group bonded to gold(I), at 1627 (vs, br) and 1192 (vs, br) cm^{-1} from trifluoroacetate, and at 1264 (s) characteristic of the tht molecule. The presence of tht is also confirmed in its ^1H NMR spectrum, which displays two multiplets at 2.21 and 3.44 ppm, and its ^{19}F NMR spectrum shows the typical pattern of a pentafluorophenyl group bonded to gold(I) and a singlet at −73.1 ppm due to trifluoroacetate. The mass spectrum of **1** using MALDI-TOF (matrix-assisted laser desorption/ionization-time of flight) technique displays peaks at m/z = 865 (100%, $[Ag_3(CF_3CO_2)_4(tht)]^-$) and 531 (65%, $[Au(C_6F_5)_2]^-$), which suggests a certain degree of association.

Scheme 1. Synthesis of Complexes 1−3

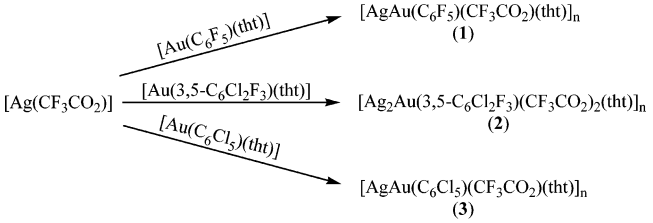

Scheme 1

When the aryl group present in the starting complex is 3,5-$C_6Cl_2F_3$, treatment of $[Au(3,5\text{-}C_6Cl_2F_3)(tht)]$ with $[Ag(CF_3CO_2)]$ in dichloromethane leads to the synthesis of a complex with a lower Au/Ag ratio: $[Ag_2Au(C_6Cl_2F_3)(CF_3CO_2)_2(tht)]_n$ (**2**). When the reaction is carried out in diethyl ether, the same complex is obtained, but in lower yield. Complex **2** is the product of the reaction independent of the molar ratio of the starting materials, which suggests that the substitution of two fluorine atoms by the less electronegative halogen chlorine leads to a more basic gold(I) reagent that binds two silver centers per gold atom. Complex **2** is isolated as a pale yellow solid stable to air and moisture and is nonconducting in acetone solutions. The analytical and spectroscopic data agree with the proposed formulation, and thus its FT-IR spectrum in Nujol mulls shows, besides the bands arising from tht and trifluoroacetate, absorptions at 1586 (s), 1556 (m), 1061 (vs), and 771 (vs) cm^{-1} due to the aryl group bonded to gold(I). Its ^1H NMR spectrum shows two multiplets at 2.21 and 3.43 ppm, corresponding to tht, and the resonances of the fluorine atoms of the trifluoroacetate and 3,5-dichlorotrifluorophenyl groups are observed in its ^{19}F NMR spectrum at −73.1 ppm, and at −89.8 and −115.9 ppm, respectively. Again, a certain degree of association in solution is suggested by the mass spectrum of **2** (MALDI-TOF), which shows peaks at m/z = 997 (27%), 865 (13%), and 597 (100%), corresponding to the fragments $[Au_2(3,5\text{-}C_6Cl_2F_3)_3]^-$, $[Ag_3(CF_3CO_2)_4(tht)]^-$, and $[Au(C_6Cl_2F_3)_2]^-$, respectively.

Finally, when all the fluorine atoms of the gold(I) starting complex are substituted by chlorine, an even lower Au/Ag would be expected in the resulting product in accordance with a more basic character of the substrate. Notwithstanding, the reaction of $[Au(C_6Cl_5)(tht)]$ with $[Ag(CF_3CO_2)]$ in diethyl ether leads to a new complex of stoichiometry $[AgAu(C_6Cl_5)(CF_3CO_2)$-

(7) (a) Contel, M.; Jiménez, J.; Jones, P. G.; Laguna, A.; Laguna, M. *J. Chem. Soc., Dalton Trans.* **1994**, 2515. (b) Contel, M.; Garrido, J.; Gimeno, M. C.; Jones, P. G.; Laguna, A.; Laguna, M. *Organometallics* **1996**, *15*, 4939. (c) Cerrada, E.; Contel, M.; Valencia, A. D.; Laguna, M.; Gelbrich, T.; Hursthouse, M. B. *Angew. Chem., Int. Ed.* **2000**, *39*, 2353. (d) Fernández, E. J.; Gimeno, M. C.; Laguna, A.; López-de-Luzuriaga, J. M.; Monge, M.; Pyykkö, P.; Sundholm, D. *J. Am. Chem. Soc.* **2000**, *122*, 7287. (e) Fernández, E. J.; Laguna, A.; López-de-Luzuriaga, J. M.; Montiel, M.; Olmos, M. E.; Pérez, J.; Puelles, R. C. *Organometallics* **2006**, *25*, 4307. (f) Fernández, E. J.; Laguna, A.; López-de-Luzuriaga, J. M.; Monge, M.; Montiel, M.; Olmos, M. E.; Pérez, J.; Puelles, R. C.; Sáenz, J. C. *J. Chem. Soc., Dalton Trans.* **2005**, 1162.

(8) (a) Usón, R.; Laguna, A.; Laguna, M.; Jones, P. G.; Sheldrick, G. M. *Chem. Commun.* **1981**, 1097. (b) Usón, R.; Laguna, A.; Laguna, M.; Jones, P. G.; Sheldrick, G. M. *J. Chem. Soc., Dalton Trans* **1984**, 285. (c) Burini, A.; Bravi, R.; Fackler, J. P., Jr.; Galassi, R.; Grant, T. A.; Omary, M. A.; Pietroni, B. R.; Staples, R. J. *Inorg. Chem.* **2000**, 39, 3158. (d) Burini, A.; Fackler, J. P., Jr.; Galassi, R.; Pietroni, B. R.; Staples, R. J. *Chem. Commun.* **1998**, 95. (e) Contel, M.; Garrido, J.; Gimeno, M. C.; Laguna, M. *J. Chem. Soc., Dalton Trans.* **1998**, 1083. (f) Usón, R.; Laguna, A.; Laguna, M.; Usón, A.; Jones, P. G.; Erdbrugger, C. F. *Organometallics* **1987**, *6*, 1778. (g) Schuster, O.; Monkowius, U.; Schmidbaur, H.; Ray, R. S.; Krüger, S.; Rösch, N. *Organometallics* **2006**, *25*, 1004.

(9) (a) Fernández, E. J.; Laguna, A.; López-de-Luzuriaga, J. M.; Monge, M.; Montiel, M.; Olmos, M. E. *Inorg. Chem.* **2007**, *46*, 2953. (b) Fernández, E. J.; Laguna, A.; López-de-Luzuriaga, J. M.; Montiel, M.; Olmos, M. E.; Pérez, J. *Organometallics* **2005**, *24*, 1631. (c) Fernández, E. J.; Laguna, A.; López de Luzuriaga, J. M.; Mendizabal, F.; Monge, M.; Olmos, M. E.; Pérez, J. *Chem.−Eur. J.* **2003**, *9*, 456. (d) Fernández, E. J.; López-de-Luzuriaga, J. M.; Monge, M.; Olmos, M. E.; Pérez, J.; Laguna, A. *J. Am. Chem. Soc.* **2002**, *124*, 5942. (e) Fernández, E. J.; Jones, P. G.; Laguna, A.; López-de-Luzuriaga, J. M.; Monge, M.; Pérez, J.; Olmos, M. E. *Inorg. Chem.* **2002**, *41*, 1056. (f) Crespo, O.; Fernández, E. J.; Jones, P. G.; Laguna, A.; López-de-Luzuriaga, J. M.; Mendía, A.; Monge, M.; Olmos, M. E. *Chem. Commun.* **1998**, 2233.

(10) Fernández, E. J.; Laguna, A.; Olmos, M. E. *Adv. Organomet. Chem.* **2005**, *52*, 77.

(11) Hollatz, C.; Schier, A.; Schmidbaur, H. *J. Am. Chem. Soc.* **1997**, *119*, 8115.

(12) Casado, A. L.; Espinet, P. *Organometallics* **1998**, *17*, 3677.

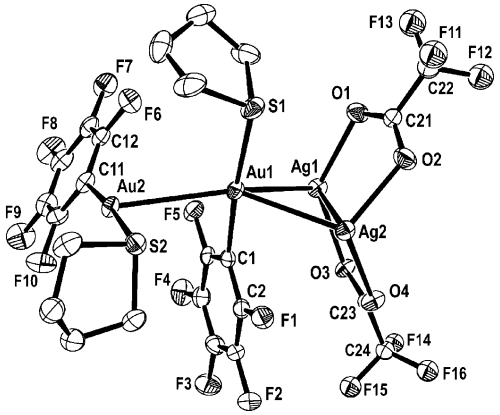

Figure 1. Asymmetric unit of the crystal structure of complex **1** (30% probability level) with the labeling scheme of the atom positions. Hydrogen atoms have been omitted for clarity.

(tht)]$_n$ (**3**), even when it is not carried out with equimolecular amounts of the reagents. Compound **3** is isolated as a white air-stable powder, and it behaves as a nonconductor in acetone solution. Its IR spectrum shows bands from the aryl group bonded to gold(I) at 843 (vs) and 628 (s) cm^{-1}, from the tht ligand at 1259 (s) cm^{-1}, and from the trifluoroacetate anion at 1643 (vs, br) and 1202 (vs, br) cm^{-1}. Its ^{1}H NMR spectrum is very similar to those of **1** and **2** and confirms the presence of tht with two multiplets at 2.20 and 3.40 ppm. The ^{19}F NMR of **3**, which shows a singlet at −73.1 ppm, indicates a similar behavior of the trifluoroacetate anion in the three complexes. Finally, its mass spectrum (MALDI-TOF) displays peaks at *m*/*z* = 1140 (10%) and 694 (100%), which correspond to the fragments $[Au_2(C_6Cl_5)_3]^-$ and $[Au(C_6Cl_5)_2]^-$, respectively.

Crystal Structures. The crystal structures of complexes **1**−**3** were determined by X-ray diffraction methods from single crystals obtained by slow diffusion of *n*-hexane into a solution of the complex in dichloromethane. They are shown in Figures 1−6; Table 1 contains details of the data collection and refinement methods, and selected bond lengths and angles are shown in Tables 2−4. Although the three crystal structures are different, they display some common features: all of them are polymers formed by the association of linear $[Au(C_6X_5)(tht)]$ units and eight-membered $[Ag_2(CF_3CO_2)_2]$ rings, assembled through Au···Ag contacts and various other interactions that depend on the aryl group.

Complex **1** crystallizes in the space group $P2_1/n$ of the monoclinic system, with two $[Au(C_6F_5)(tht)]$ units and an $[Ag_2(CF_3CO_2)_2]$ cycle in the asymmetric unit connected through short metal−metal contacts (Figure 1). Au(1) is bonded to both silver atoms of the $[Ag_2(CF_3CO_2)_2]$ fragment in the asymmetric unit and also to Au(2), with Au−Ag and Au−Au bond distances of 2.8792(5) and 2.9029(5) Å, and 3.0845(3) Å, respectively, all intermetallic contacts being unsupported. By contrast, Au(2) is bonded to Au(1) and to only one silver center of a neighboring dimetallacycle (via the 2_1 screw axis) with an Au−Ag distance of 2.8963(6) Å. This last interaction is bridged by the *ipso* carbon atom of the aryl group bonded to Au(2) (Ag−C = 2.684(6) Å), although this fact does not influence the intermetallic distance. These are in general comparable to those found in the related derivatives $[AuAg_4(mes)(CF_3CO_2)_4(tht)]_n$ (mes = mesityl) (2.8226(4) and 2.8993(4) Å), $[AuAg_4(mes)(CF_3CF_2CO_2)_4(tht)_3]_n$ (2.8540(6), 2.8845(6), and 3.0782(6) Å), $\{[AuAg_4(mes)(CF_3CO_2)_4(tht)(H_2O)]\cdot H_2O\cdot CH_2Cl_2\}_n$ (2.8505(6), 2.8708(6), and 3.1347(7) Å),[7e] or $(NBu_4)_2[Au(3,5\text{-}C_6F_3Cl_2)_2Ag_4(CF_3CO_2)_5]$ (2.9010(6)−3.0134(6) Å)[7f] and longer than in

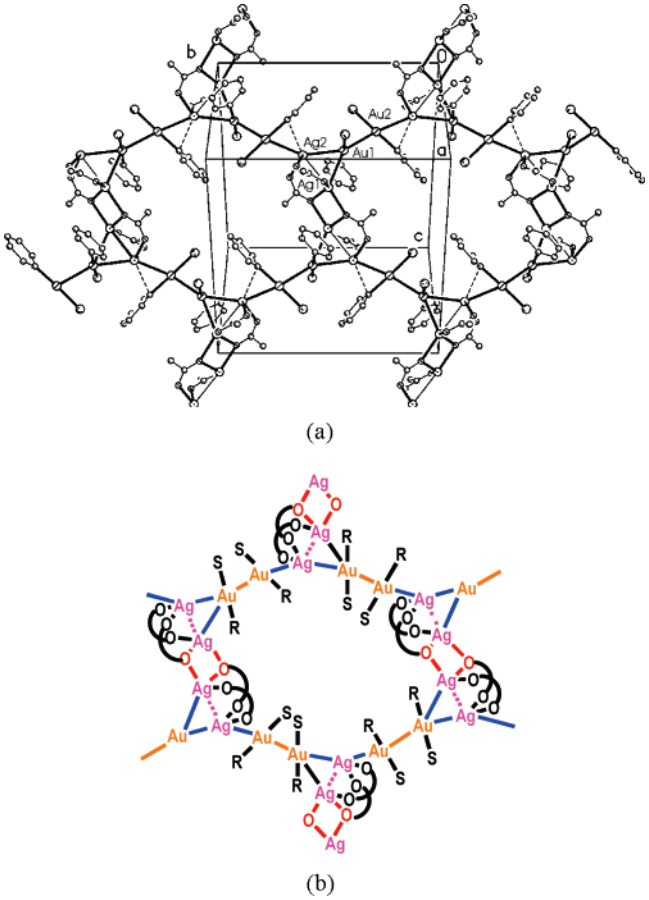

Figure 2. (a) Two-dimensional structure of complex **1**. Hydrogen, fluorine, and the carbon atoms of tht have been omitted for clarity. (b) Schematic drawing of the polymeric structure of **1**. Ag···Ag, Au···Ag, Au···Au, and Ag−O···Ag contacts responsible for the polymerization are highlighted in purple, blue, orange, and red, respectively.

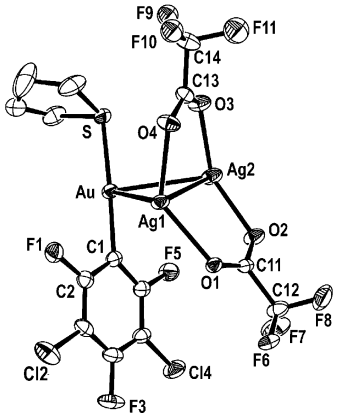

Figure 3. Asymmetric unit of the crystal structure of complex **2** (30% probability level) with the labeling scheme of the atom positions. Hydrogen atoms have been omitted for clarity.

$[AuAg_4(mes)(CF_3CF_2CO_2)_4(tht)]_n$ (2.8140(8) and 2.8166(8) Å)[7e] or in most of the complexes containing aryl bridging ligands between gold and silver (2.7758(8)−2.8245(6) Å).[7]

The Ag(I) atoms of the dimeric $[Ag_2(CF_3CO_2)_2]$ unit display an Ag···Ag contact of 2.8963(6) Å, similar to those found in most analogous structures of complexes of the type $[Ag_2(RCO_2)_2L_n]$ (n = 1, 2) (from 2.8669(9) to 3.3813(6) Å)[13] but slightly shorter than those described in the related mesityl derivatives $[AuAg_4(mes)(RCO_2)_4(tht)_x]_n$ (R = CF_3, x = 1; R =

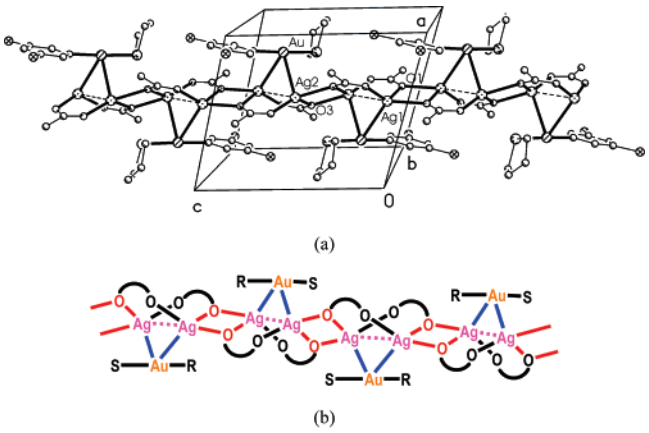

Figure 4. (a) One-dimensional structure of complex **2**. Hydrogen, chlorine, and fluorine atoms have been omitted for clarity. (b) Schematic drawing of the polymeric structure of **2**. Au···Ag, Ag···Ag, and Ag−O···Ag contacts responsible for the polymerization are highlighted in blue, purple, and red, respectively.

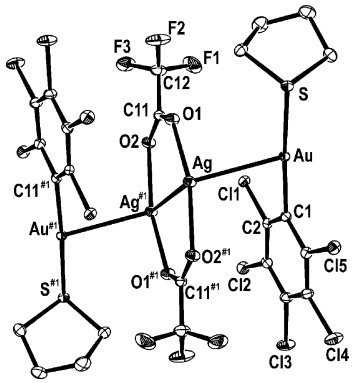

Figure 5. Crystal structure of complex **3** (30% probability level) with the labeling scheme of the atom positions. Hydrogen atoms have been omitted for clarity.

CF_3CF_2, $x = 1$, 3) or $\{[AuAg_4(mes)(CF_3CO_2)_4(tht)(H_2O)]\cdot H_2O\cdot CH_2Cl_2\}_n$ (2.9149(5)−3.0958(7) Å).[7e]

The gold(I) centers display their usual linear environment by coordination to the *ipso* carbon atom of an aryl group with typical Au−C bond lengths of 2.050(6) and 2.039(6) Å and to the sulfur of a tht molecule with Au−S distances of 2.3260(19) and 2.3184(16) Å, shorter than in $[AuAg_4(mes)(CF_3CF_2CO_2)_4(tht)_3]_n$ (2.3423(16) Å) or in $\{[AuAg_4(mes)(CF_3CO_2)_4(tht)(H_2O)]\cdot H_2O\cdot CH_2Cl_2\}_n$ (2.3386(19) Å),[7e] where the S-donor ligand has a similar structural disposition. If the Ag···Ag contact is not considered, each silver center displays a pyramidal environment (see Table 2) by coordination to Au(1) and two oxygen atoms of the trifluoroacetate anions with Ag−O distances in the range 2.258(5)−2.339(4) Å. The pyramidal geometry within the asymmetric unit is extended to distorted tetrahedral by the additional bonds Au2···Ag2#1 and Ag1−O3#2 (see below).

(13) (a) Powell, J.; Horvath, M. J.; Lough, A.; Phillips, A.; Brunet, J. *J. Chem. Soc., Dalton Trans.* **1998**, 637. (b) Che, C.-M.; Tse, M-C.; Chan, M. C. W.; Cheung, K.-K.; Phillips, D. L.; Leung, K.-H. *J. Am. Chem. Soc.* **2000**, *122*, 2464. (c) Tsuchiya, T.; Shimizu, T.; Hirabayashi, K.; Kamigata, N. *J. Org. Chem.* **2002**, *67*, 6632. (d) Brandys, M. C.; Puddephatt, R. J. *J. Am. Chem. Soc.* **2002**, *124*, 3946. (e) Brammer, L.; Burgard, M. D.; Eddleston, M. D.; Rodger, C. S.; Rath, N. P.; Adams, H. *Cryst. Eng. Commun.* **2004**, *44*, 239. (f) Djordjevic, B.; Schuster, O.; Schmidbaur, H. *Inorg. Chem.* **2005**, *44*, 673. (g) Zhong, J. C.; Munakata, M.; Maekawa, M.; Kuroda-Sowa, T.; Suenaga, Y.; Konaka, H. *Inorg. Chim. Acta* **2003**, *342*, 202. (h) Schultheiss, N.; Powell, D. R.; Bosch, E. *Inorg. Chem.* **2003**, *42*, 5304. (i) Bosch, E.; Barnes, C. L. *Inorg. Chem.* **2002**, *41*, 2543. (j) Awaleh, M. O.; Badia, A.; Brisse, F.; Bu, X.-H. *Inorg. Chem.* **2006**, *45*, 1560.

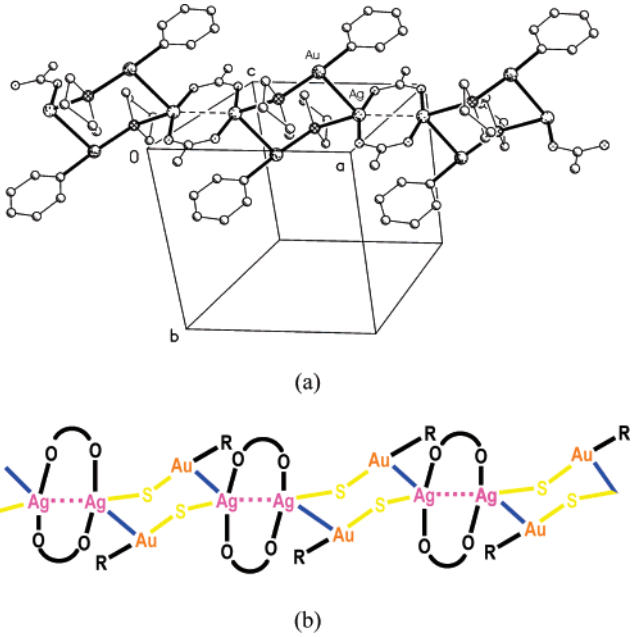

Figure 6. (a) One-dimensional structure of complex **3**. Hydrogen and chlorine atoms have been omitted for clarity. (b) Schematic drawing of the polymeric structure of **3**. Au···Ag, Ag···Ag, and Au−S···Ag contacts responsible for the polymerization are highlighted in blue, purple, and yellow, respectively.

The above-mentioned unsupported Au···Au and Au···Ag interactions are responsible for the polymerization of these units into infinite chains with backbone $(-Au2-Au1-Ag2-)_n$ parallel to the *y*-axis. The chains are interconnected through cross-links consisting of trifluoroacetates and central, inversion-symmetric four-membered rings $Ag(1)_2O(3)_2$, thus resulting in a two-dimensional polymer parallel to 101, as shown in Figure 2. The bridging Ag1−O3#2 distance of 2.382(4) Å is slightly longer than the Ag−O lengths within the dimeric $[Ag(CF_3CO_2)]_2$ unit and nearly identical to one of the Ag−O distances (2.398(6) Å) found in $\{[Ag_2(CH_3CN)_2][L^{Ir}]_2(OTf)_2\}_n$ (L^{Ir} = [Cp*Ir(η^4-benzoquinone)]), where Ag_2O_2 rings are also responsible for the polymerization of the complex.[14]

As noted in the Synthesis and Characterization section, the Au/Ag ratio in **2** is lower than in **1**, and thus the asymmetric unit of the crystal structure of **2** (Figure 3) contains only one (instead of two) [Au(3,5-$C_6Cl_2F_3$)(tht)] fragment together with an $[Ag_2(CF_3CO_2)_2]$ ring. These units are connected through unsupported Au···Ag interactions of 2.8784(5) and 3.0221(6) Å, the latter somewhat longer than in complex **1** (2.8792(5), 2.9029(5), and 2.8963(6) Å) and both of them in general longer than those observed for other complexes displaying unsupported Au···Ag contacts.[8] The Ag−Ag distance within the $[Ag_2(CF_3CO_2)_2]$ unit is 2.8623(6) Å, slightly shorter than in **1** (2.8963(6) Å) and also shorter than in the related Au/Ag mesityl derivatives $[AuAg_4(mes)(RCO_2)_4(tht)_x]_n$ (R = CF_3, $x = 1$; R = CF_3CF_2, x = 1,3) or $\{[AuAg_4(mes)(CF_3CO_2)_4(tht)(H_2O)]\cdot H_2O\cdot CH_2Cl_2\}_n$ (2.9149(5)−3.0958(7) Å).[7e] Thus, the three metal centers form a nearly equilateral triangle.

The [Au(3,5-$C_6Cl_2F_3$)(tht)] unit shows a linear environment for gold with Au−C and Au−S bond lengths of 2.024(6) and 2.3159(15) Å, respectively, both of them shorter than in complex **1**, and the latter also shorter than in the related compounds $[AuAg_4(mes)(CF_3CF_2CO_2)_4(tht)_3]_n$ (2.3423(16) Å) and $\{[AuAg_4(mes)(CF_3CO_2)_4(tht)(H_2O)]\cdot H_2O\cdot CH_2Cl_2\}_n$ (2.3386(19)

(14) Moussa, J.; Guyard-Duhayon, C.; Boubekeur, K.; Amouri, H.; Yip, S.-K.; Yam., V. W. W. *Cryst. Growth Des.* **2007**, *7*, 962.

Table 1. Data Collection and Structure Refinement Details for Complexes 1−3

	1	2	3
chemical formula	$C_{24}H_{16}Ag_2Au_2F_{16}O_4S_2$	$C_{14}H_8Ag_2AuCl_2F_9O_4S$	$C_{12}H_8AgAuCl_5F_3O_2S$
cryst habit	pale yellow prism	yellow prism	colorless tablet
cryst size/mm	0.25 × 0.25 × 0.15	0.20 × 0.20 × 0.18	0.20 × 0.16 × 0.07
cryst syst	monoclinic	triclinic	triclinic
space group	$P2_1/n$	$P\bar{1}$	$P\bar{1}$
a/Å	12.432(2)	10.280(2)	8.6735(6)
b/Å	15.526(3)	10.444(2)	9.4223(6)
c/Å	16.748(4)	11.073(2)	12.1291(8)
α/deg	90	97.187(10)	77.492(3)
β/deg	92.464(10)	104.066(10)	73.345(3)
γ/deg	90	104.095(10)	82.557(3)
V/Å^3	3229.69(11)	1096.84(4)	924.70(11)
Z	4	2	2
D_c/g cm^{-3}	2.769	2.806	2.713
M	1346.16	926.87	755.33
F(000)	2480	856	700
T/°C	−173	−173	−173
$2\theta_{max}$/deg	56	56	62
μ(Mo Kα)/mm^{-1}	10.506	8.874	9.851
no. of reflns measd	26 327	18 076	38 148
no. of unique reflns	7580	5225	5983
R_{int}	0.0490	0.0452	0.0223
R^a ($I > 2\sigma(I)$)	0.0368	0.0348	0.0122
wR^b (F^2, all reflns)	0.0756	0.0835	0.0304
no. of params	480	328	226
no. of restraints	132	37	18
S^c	1.032	1.040	1.097
max. $\Delta\rho$/e Å^{-3}	1.835	2.977	2.229

[a] $R(F) = \sum||F_o| - |F_c||/\sum|F_o|$. [b] $wR(F^2) = [\sum\{w(F_o^2 - F_c^2)^2\}/\sum\{w(F_o^2)^2\}]^{0.5}$; $w^{-1} = \sigma^2(F_o^2) + (aP)^2 + bP$, where $P = [F_o^2 + 2F_c^2]/3$ and a and b are constants adjusted by the program. [c] $S = [\sum\{w(F_o^2 - F_c^2)^2\}/(n - p)]^{0.5}$, where n is the number of data and p the number of parameters.

Table 2. Selected Bond Lengths [Å] and Angles [deg] for Complex 1[a]

Au(1)−C(1)	2.050(6)
Au(1)−S(1)	2.3260(19)
Au(1)−Ag(1)	2.8792(5)
Au(1)−Ag(2)	2.9029(5)
Au(1)−Au(2)	3.0845(3)
Au(2)−C(11)	2.039(6)
Au(2)−S(2)	2.3184(16)
Au(2)−Ag(2)#1	2.8135(5)
Ag(1)−O(1)	2.258(5)
Ag(1)−O(3)	2.334(4)
Ag(1)−O(3)#2	2.382(4)
Ag(1)−Ag(2)	2.8963(6)
Ag(2)−O(2)	2.303(5)
Ag(2)−O(4)	2.339(4)
Ag(2)−C(11)#3	2.684(6)
C(1)−Au(1)−S(1)	174.95(15)
C(11)−Au(2)−S(2)	174.93(18)
O(1)−Ag(1)−O(3)	135.18(17)
O(1)−Ag(1)−Au(1)	96.59(14)
O(3)−Ag(1)−Au(1)	114.67(11)
O(2)−Ag(2)−O(4)	106.1(2)
O(2)−Ag(2)−Au(1)	107.29(13)
O(4)−Ag(2)−Au(1)	115.24(11)

[a] Symmetry transformations used to generate equivalent atoms: #1 $-x+1/2,y-1/2,-z+1/2$; #2 $-x,-y+2,-z$; #3 $-x+1/2,y+1/2,-z+1/2$.

Table 3. Selected Bond Lengths [Å] and Angles [deg] for Complex 2[a]

Au−C(1)	2.026(6)
Au−S	2.3158(16)
Au−Ag(1)	2.8784(5)
Au−Ag(2)	3.0221(6)
Ag(1)−Ag(2)	2.8623(6)
Ag(1)−O(4)	2.247(4)
Ag(1)−O(1)	2.324(4)
Ag(1)−O(1)#1	2.401(4)
Ag(2)−O(2)	2.191(4)
Ag(2)−O(3)	2.301(4)
Ag(2)−O(3)#2	2.390(4)
C(1)−Au−S	177.58(15)
O(4)−Ag(1)−O(1)	132.66(17)
O(4)−Ag(1)−Au	98.34(12)
O(1)−Ag(1)−Au	111.38(10)
O(2)−Ag(2)−O(3)	137.89(19)
O(2)−Ag(2)−Au	116.57(13)
O(3)−Ag(2)−Au	89.13(13)

[a] Symmetry transformations used to generate equivalent atoms: #1 $-x+1,-y+1,-z$; #2 $-x+1,-y+1,-z+1$.

Å),[7e] which also contain terminal tht ligands. As in the crystal structure of compound **1**, each Ag(I) center displays a pyramidal environment without considering the Ag···Ag contact (see Table 3) by coordination to a gold center and to two oxygen atoms of the CF_3 anions with Ag−O distances ranging from 2.191(4) to 2.324(4) Å. The coordination geometry is extended to distorted tetrahedral by the additional Ag−O bonds to other asymmetric units (see below).

The main difference between this structure and the one described above for **1** is the absence of aurophilic interactions in this species, the shortest Au−Au distance being greater than 7 Å. Consequently, the polymerization in this case takes place only through Ag−O−Ag bridges between the silver dimers, forming inversion-symmetric four-membered Ag_2O_2 rings and resulting in chains that run parallel to the crystallographic z-axis (Figure 4). The Ag−O distances responsible for the polymerization, of 2.401(4) and 2.390(4) Å, are longer than those within the $[Ag(CF_3CO_2)]_2$ unit (2.191(4) to 2.324(4) Å).

The stoichiometry of complex **3** was unequivocally established in its crystal structure, which, as in **1**, shows a 1:1 gold:silver ratio. Nevertheless, the structure is different from that of complex **1**; it crystallizes in the space group $P\bar{1}$ with one [Au(C_6Cl_5)(tht)] unit and a half of an $[Ag_2(CF_3CO_2)_2]$ cycle in the asymmetric unit (Figure 5). The gold center in **3** binds only one silver(I) atom, whereas in **2** there are two Au···Ag interactions, and in **1** two Au···Ag and one Au···Au contact are present. The Au−Ag distance of 2.96615(19) Å is longer than most of the Au−Ag distances in **1** and **2** and also longer

Table 4. Selected Bond Lengths [Å] and Angles [deg] for Complex 3[a]

Au−C(1)	2.0296(15)
Au−S	2.3109(4)
Au−Ag	2.96615(19)
Ag−O(1)	2.2026(12)
Ag−O(2)#1	2.2421(12)
Ag−S#2	2.7033(4)
Ag−Ag#1	3.0071(3)
C(1)−Au−S	176.09(4)
O(1)−Ag−O(2)#1	159.97(4)
O(1)−Ag−S#2	109.91(3)
O(2)#1−Ag−S#2	85.50(3)
O(1)−Ag−Au	92.25(3)
O(2)#1−Ag−Au	101.92(3)
S#2−Ag−Au	85.560(10)
Au−S−Ag#2	122.104(16)

[a] Symmetry transformations used to generate equivalent atoms: #1 $-x,-y,-z+1$; #2 $-x+1,-y,-z+1$.

than most of the unsupported Au···Ag contacts observed for other complexes.[8]

The gold(I) atom is again linearly coordinated to the *ipso* carbon atom of an aryl group with a typical Au−C bond length of 2.0296(15) Å and to the sulfur of a tht molecule with an Au−S distance of 2.3109(4) Å. A significant difference between the crystal structure of **3** and those described for **1** and **2** is that the sulfur atom of the tht in **3** acts as electron density donor not only to a Au(I) center of the [Au(C_6Cl_5)(tht)] unit but also to an Ag(I) atom of an adjacent [$Ag_2(CF_3CO_2)_2$] dimer, thus forming, together with the Au···Ag contacts, hexanuclear $Ag_2Au_2S_2$ rings (see Figure 6) similar to those recently reported by us in complexes [$AuAg_4$(mes)$(RCO_2)_4$(tht)]$_n$ (R = CF_3, CF_3CF_2).[7e] However, the Au−S bond length is shorter than in both mesityl derivatives (2.3195(11) Å for R = CF_3, 2.347(2) Å for R = CF_3CF_2) or in other complexes with gold(I) bonded to a terminal tht (2.237−2.335(6) Å),[15] slightly shorter than in complex **1** (2.3260(19) and 2.3184(16) Å), and similar to that in **2** (2.3159(15) Å), although in these last cases the tht molecule acts as a terminal instead of a bridging ligand and a stronger interaction would be expected. The Ag−S distance of 2.7033(4) Å is in this case shorter than in [$AuAg_4$(mes)$(CF_3CF_2CO_2)_4$(tht)]$_n$ (2.888(2) Å),[7e] but longer than in other complexes, such as [$AuAg_4$(mes)$(CF_3CO_2)_4$(tht)]$_n$ (2.6877(11) Å),[7e] [$Ag_4(CF_3CO_2)_4$(tht)$_2$] (2.4420(8) Å),[7e] [$Ag(O_3SCF_3)(SC_4H_8)$]$_n$[16] (2.4897(9) and 2.4963(9) Å), and [{(Ph_3P)Au(μ-mes)Ag(SC_4H_8)}$_2$][SO_3CF_3]$_2$[7a] (2.8245(6) Å).

As in the crystal structures of **1** and **2**, the Ag(I) atoms of the dimeric [$Ag_2(CF_3CO_2)_2$] units in **3** show Ag···Ag contacts of 3.0071(3) Å, weaker than in **1** and **2**. The Ag−O distances within the dimer, of 2.2026(12) and 2.2421(12) Å, are comparable to those found in complexes **1** and **2**. The trifluoroacetate anions and the argentophilic contacts link neighboring $Ag_2Au_2S_2$ rings, leading to the formation of a monodimensional polymer parallel to the *x*-axis, as shown in Figure 6.

Optical Properties. All the presented gold−silver complexes are luminescent in solid state at room temperature and at 77 K or in frozen solutions (dichloromethane or acetone) (see Table 5). The optical behavior in frozen solution is similar for the three complexes, but not in the solid state. Thus, for example, the experimental emission values for compounds **1**−**3** in dichloromethane at 77 K appear in the same region of energy, at 485 (exc. 390) for **1**, 495 (exc. 370) for **2**, and 505 (350 nm) for **3**, similar also to the three precursor gold complexes [AuR(tht)], which show emissions at 485 (exc. 370; R = C_6F_5), 495 (exc. 370; R = $C_6Cl_2F_3$), and 505 nm (exc. 380; R = C_6Cl_5) (Table 6).

By contrast, the mixed-metal complexes and the gold precursors show different emissions in the solid state. In the latter, a bathochromic shift is observed at room temperature as the electronegativity of the aryl substituents decreases (Table 6), but for complexes **1**−**3** (see Figure 7) the same sequence is not observed, suggesting different origins. In addition, complex **1** displays two emissions at 77 K, which is not observed for the rest of the derivatives or for complex **3**, whose emission is red-shifted under pressure to 564 nm, a fact that could be related to a phase exchange.[17] The lifetimes of the emissions in the solid state at room temperature are in the microsecond range, suggesting phosphorescent processes in all cases.

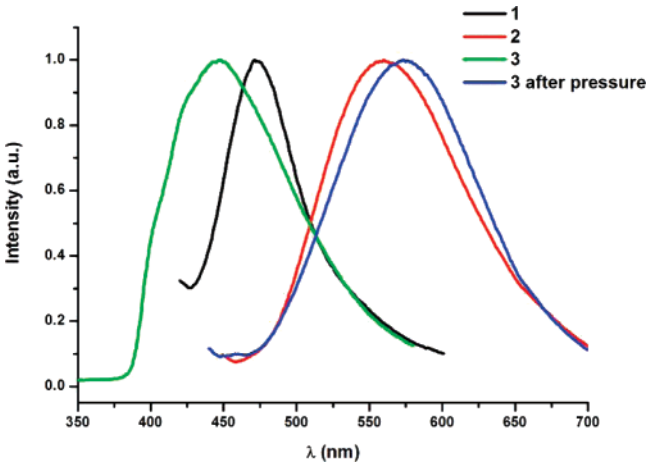

Figure 7. Emission spectra for complexes **1**−**3** in the solid state at room temperature.

Table 5. Spectroscopic and Photophysical Properties of 1−3

complex	medium (T [K])	λ_{em} (λ_{exc}) [nm]/τ (μs)
1	CH_2Cl_2 (77)	485 (390)
	solid (298)	473 (378)/8.3
	solid (77)	430, 480 (385)/11.6, 12.1
2	CH_2Cl_2 (77)	495 (370)
	solid (298)	570 (410)/7.9
	solid (77)	590 (490)
3	CH_2Cl_2 (77)	505 (350)
	solid (298)	447 (307)/57.0
		564 (423) pressure
	solid (77)	495 (300)
		550 (405) pressure

Table 6. Spectroscopic and Photophysical Properties of Gold Precursors

complex	medium (T [K])	λ_{em} (λ_{exc}) [nm]
[Au(C_6F_5)(tht)]	CH_2Cl_2 (77)	482 (370)
	solid (298)	414 (300)
	solid (77)	460 (360)
[Au($C_6F_3Cl_2$)(tht)]	CH_2Cl_2 (77)	484 (370)
	solid (298)	428 (300)
	solid (77)	443 (360)
[Au(C_6Cl_5)(tht)]	CH_2Cl_2 (77)	481 (380)
	solid (298)	467 (300)
	solid (77)	477 (363)

(15) (a) Ahrland, S; Noren, B.; Oskarsson, A. *Inorg. Chem.* **1985**, *24*, 1330. (b) Friedrichs, S.; Jones. P. G. *Acta Crystallogr., Sect. C: Cryst. Struct. Commun.* **2000**, *56*, 56. (c) López de Luzuriaga, J. M.; Schier, A.; Schmidbaur, H. *Chem. Ber.* **1997**, *130*, 647. (d) Ahrens, B.; Jones, P. G. *Z. Naturforsch., B: Chem. Sci.* **2000**, *55*, 803. (e) Ahrland, S.; Dreisch, K.; Noren, B. Oskarsson, A. *Mater. Chem. Phys.* **1993**, *35*, 281. (f) Abdou, H. E.; Mohammed, A. A.; Fackler, J. P., Jr. *Inorg. Chem.* **2005**, *44*, 166.

(16) Bardají, M.; Crespo, O.; Laguna, A.; Fischer, A. K. *Inorg. Chim. Acta* **2000**, *304*, 7.

(17) (a) Moses, D.; Feldblum, A.; Ehrenfreund, E.; Heeger, A. J.; Chung, T. C.; MacDiarmid, A. G. *Phys. Rev. B* **1982**, *26*, 3361. (b) Zhao, X.; Schroeder, J.; Bilodeau, T. G.; Hwa, L. *Phys. Rev. B* **1989**, *40*, 1257.

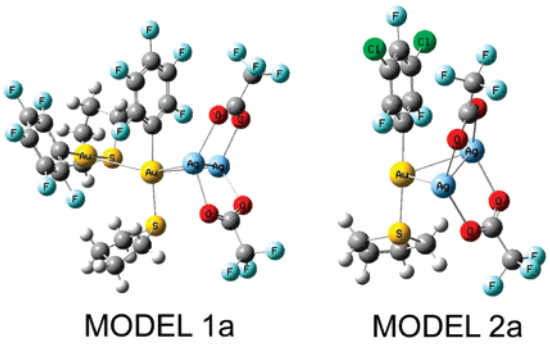

Figure 8. Theoretical model systems $[Au_2Ag_2(C_6F_5)_2(CF_3CO_2)_2(tht)_2]$ (**1a**) and $[AuAg_2(C_6F_3Cl_2)_2(CF_3CO_2)_2(tht)]$ (**2a**).

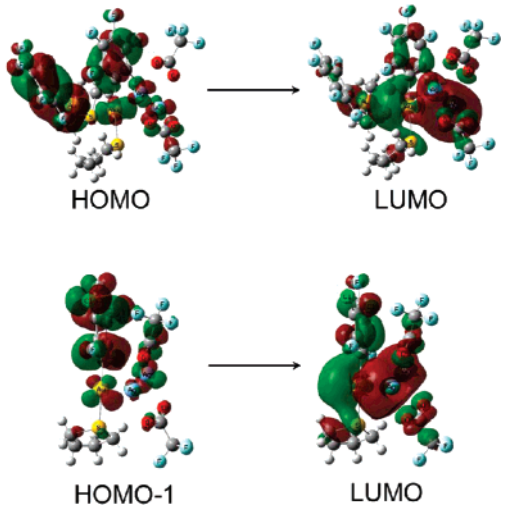

Figure 9. Most important contributions to the lowest triplet transitions (T_1) for model systems $[Au_2Ag_2(C_6F_5)_2(CF_3CO_2)_2(tht)_2]$ (**1a**) and $[AuAg_2(C_6F_3Cl_2)_2(CF_3CO_2)_2(tht)]$ (**2a**).

We have also carried out DFT and TDDFT calculations on simplified model systems for complexes **1**−**3**. For complex **1** we have chosen the model $[Au_2Ag_2(C_6F_5)_2(CF_3CO_2)_2(tht)_2]$ (**1a**), and for complexes **2** and **3** we have used model systems $[AuAg_2R(CF_3CO_2)_2(tht)]$ (R = $C_6F_3Cl_2$ (**2a**) and C_6Cl_5 (**2b**)) (Figure 8). In all cases we have included all the metallophilic interactions observed experimentally. From DFT calculations the nature of the frontier orbitals can be analyzed. In general, the highest occupied molecular orbitals are mostly placed at the perhalophenyl groups with some contribution from the gold centers, especially for model **1a**, in which a gold···gold interaction is involved. The lowest unoccupied molecular orbitals are mainly located at gold and silver centers (see Supporting Information).

TDDFT calculations permit an estimate of the energy of the lowest triplet excitations and the orbitals that contribute to them. For model **1a** we have calculated the two lowest triplet excitations since two phosphorescent emissions are observed experimentally. Thus, the calculated energy for T_1 is 380 nm and for T_2 is 369 nm, meanwhile the observed excitation spectra for complex **1** at room temperature displays a band at 385 nm, in agreement with the theoretical results. We have also calculated the lowest triplet excitation for models **2a** and **3a**, displaying theoretical values of 385 and 406 nm, in close agreement with the experimental values of 410 and 423 nm, respectively (Figure 9). As we can observe, such theoretical excitations as the experimental ones follow the same trend in energy (**1** > **2** > **3**) in accordance with the higher attracting abilities of C_6F_5 > $C_6F_3Cl_2$ > C_6Cl_5 groups, indicating, perhaps, the influence of these groups in the transitions responsible for the emissions.

The fact that the luminescence in the solid state is different for complexes **1**−**3** seems to be related to the different number and types of metal−metal interactions that appear in the complexes. For instance, while complex **1** shows one Au(I)···Au(I) and two Au(I)···Ag(I) interactions, complex **2** displays just two Au(I)···Ag(I) and complex **3** shows only one Au(I)···Ag(I) interaction. Therefore the presence in the solid state at 77 K for complex **1** of two emissions at 430 and 480 nm could be related to the two different types of metallophilic interactions. Both of them have lifetimes of ca. 12 μs, in accordance with emissions arising from states of triplet parentage. Thus, we have carried out TDDFT calculations of the two lowest triplet excitations on a simplified model system, $[Au_2Ag_2(C_6F_5)_2(CF_3CO_2)_2(tht)_2]$, which includes all the metal−metal interactions. In this way we can estimate the orbitals involved in the transitions responsible for the luminescence observed for **1**. The lowest triplet excitation T_1 involves HOMO and LUMO orbitals that display a (pentafluorophenyl−gold)$_2$ character and gold−silver character, respectively (Figure 9). Therefore, this transition can be considered as a charge transfer between the $Au(C_6F_5)$ groups and the metal centers. In this regard, a similar result was obtained for Au_2M_2 (M = Ag, Cu) tetranuclear systems, in which the presence of two adjacent gold centers contributes jointly to the origin of the electronic transition, the heterometals bonded to them acting as receptors for this electronic density.[18] The second lowest triplet excitation T_2 involves mainly orbitals HOMO−3 and HOMO−5 as occupied orbitals with a high contribution from the pentafluorophenyl and trifluoroacetate groups and LUMO orbital which is placed at the metal centers. In this case ligands to metal charge transfer is suggested (see Supporting Information). Previously reported studies on luminescent Au−Ag complexes point out that the presence of metal−metal interactions influences the emission energies, intensities, and behavior at different temperatures of the isolated derivatives.[19]

In the case of the other two complexes, **2** and **3**, the triplet transition shows a similar charge transfer character from the $Au(C_6F_5)$ unit to the metals. In this case the observation of a single triplet emission can be in accordance with the presence of Au(I)···Ag(I) interactions and the absence of Au(I)···Au(I) ones and in agreement with the experimental one (Figure 9). According to these results, it seems plausible that, in addition to the triplet emission that appears as a consequence of the Au···Ag interaction, when an additional aurophilic interaction is present (e.g., complex **1**), both gold centers cooperatively contribute to another, different transition to the acidic silver atom(s), leading to another triplet emission.

It is worth mentioning that these theoretical model systems, which include the repetition units of the extended structures of **1**−**3**, give a qualitative explanation of the photophysical properties in the solid state, although the calculations on tetra-

(18) Fernández, E. J.; Laguna, A.; López-de-Luzuriaga, J. M.; Monge, M.; Montiel, M.; Olmos, M. E.; Rodríguez-Castillo, M. *Organometallics* **2006**, *25*, 3639.

(19) (a) Fernández, E. J.; Laguna, A.; López-de-Luzuriaga, J. M. *Dalton Trans.* **2007**, 1969. In particular, the following gives an example of the luminescence thermochromism due to the Au···Ag interactions present: (b) Mohammed, A. A.; Burini, A.; Fackler, J. P., Jr. *J. Am. Chem. Soc.* **2005**, *127*, 5012. The following reports an example of enhanced intensity of the emissions due to the presence of Au···Ag interactions: (c) Catalano, V. J.; Malwitz, M. A.; Etogo, A. O. *Inorg. Chem.* **2004**, *43*, 5714. (d) Wang, Q.-M.; Lee, Y.-A.; Crespo, O.; Deaton, J.; Tang, C.; Gysling, H. J.; Gimeno, M. C.; Larraz, C.; Villacampa, M. D.; Laguna, A.; Eisenberg, R. *J. Am. Chem. Soc.* **2004**, *126*, 9488.

and trinuclear compounds may not reflect the electronic structures for the more highly associated systems in the solid state. In this regard, complex **2** shows a very low-energy emission compared to those observed for complexes **1** and **3**. Although the calculations point out the same type of orbitals as responsible for the transition that leads to the emissions, the reason for this difference could be related to the different extended structures observed in the solid state. Thus, while in the case of complexes **1** and **3** the $[Au(C_6X_5)(tht)]$ units are involved in the extension of the structures through additional Au(I)···Au(I) (**1**) and S···Ag (**2**) interactions in complex **2**, the $[Au(C_6X_5)(tht)]$ units act as donors only through the gold centers. In fact, very different emissions in compounds with the same perhalophenyl groups, metal atoms, and ancillary ligands have been recently reported and justified in terms of the very different structural arrangements found in the solid state.[20]

The behavior in solution is completely different since, as we have commented on, the complexes **1**−**3** and the gold precursors show similar emission energies at 77 K in dichloromethane, but at room temperature none of them show luminescence. This fact could be related to the rupture of the metal−metal interactions in solution, which are responsible for the luminescent behavior in the solid state and are not recovered even at 77 K. An increase of the concentrations for the three complexes does not affect the luminescence energy, and only an increase of the intensity of the emissions is observed, which is indicative of the absence of aggregation in solution.

The trend of the emissions in solution is consistent with a lower energy difference in the HOMO−LUMO gap as the electronegativity of the perhalophenyl substituents decrease ($C_6F_5 > C_6F_3Cl_2 > C_6Cl_5$), and therefore, these transitions are likely to be related to $\pi\pi^*$ transitions at the perhalophenyl groups or charge transfer transitions between these groups and the gold center. The possibility of the tht ligand being responsible for this luminescent behavior can be ruled out since it is luminescent at a different energy (400 nm) as a consequence of a $n \rightarrow \sigma^*$ transition.[21]

Experimental Section

Instrumentation. Infrared spectra were recorded in the 4000−200 cm^{-1} range on a Nicolet Nexus FT-IR using Nujol mulls between polyethylene sheets. C, H, S analyses were carried out with a Perkin-Elmer 240C microanalyzer. MALDI-TOF spectra were recorded in a Microflex MALDI-TOF Bruker spectrometer operating in the linear and reflector modes using dithranol as matrix. ^1H and ^{19}F NMR spectra were recorded on a Bruker ARX 300 in $CDCl_3$ solutions. Chemical shifts are quoted relative to $SiMe_4$ (^1H, external) and $CFCl_3$ (^{19}F, external). Excitation and emission spectra were recorded with a Jobin-Yvon Horiba Fluorolog 3-22 Tau-3 spectrofluorimeter. Phosphorescence lifetime was recorded with a Fluoromax phosphorimeter accessory containing a UV xenon flash tube with a flash rate between 0.05 and 25 Hz. The lifetime data were fitted using the Jobin-Yvon software package and the Origin 6.1 program.

General Comments. Silver trifluoroacetate is commercially available and was purchased from Sigma-Aldrich. The precursor complexes [AuR(tht)] ($R = C_6F_5$, $C_6Cl_2F_3$,C_6Cl_5) were obtained according to literature procedures.[22]

Synthesis of $[AuAg(C_6F_5)(CF_3CO_2)(tht)]_n$ (1). To a solution of $[Au(C_6F_5)(tht)]$ (0.090 g, 0.2 mmol) in diethyl ether (20 mL) was added $[Ag(CF_3CO_2)]$ (0.044 g, 0.2 mmol). After 30 min of stirring the solution was concentrated under vacuum to ca. 5 mL. Addition of *n*-hexane (10 mL) led to precipitation of complex **1** as a white solid. Yield: 0.110 g (81.9%). Anal. (%) Calcd for **1** ($C_{12}H_8AuAgF_8O_2S$): C 21.41, H 1.20, S 4.76. Found: C 21.35, H 1.20, S 4.61. ^1H NMR (75.5 MHz, $CDCl_3$, ppm): δ 3.44 (m, 4H, S−CH_2−CH_2−) and 2.21 (m, 4H, S−CH_2−CH_2−). ^{19}F NMR (282.4 MHz, $CDCl_3$, ppm): δ −115.6 (m, 2F, F_o), −157.7 (t, 1F, F_p, $^3J(F_p-F_m) = 18.4$ Hz), −162.0 (m, 2F, F_m), −73.1 (s, 3F, $CF_3CO_2^-$). (MALDI-TOF −): *m*/*z* 865 ($[Ag_3(CF_3CO_2)_4(tht)]^-$ 100%), 531 ($[Au(C_6F_5)_2]^-$ 52%). FT-IR (Nujol): $\nu(C_6F_5)$ at 1504, 981 and 796 cm^{-1}, ν(tht) at 1264 cm^{-1} and $\nu(CF_3CO_2)$ at 1627 and 1192 cm^{-1}.

Synthesis of $[AuAg_2(C_6Cl_2F_3)(CF_3CO_2)_2(tht)]_n$ (2). A solution of $[Au(C_6Cl_2F_3)(tht)]$ (0.097 g, 0.2 mmol) and $[Ag(CF_3CO_2)]$ (0.088 g, 0.4 mmol) in dichloromethane (20 mL) was stirred for 30 min. The colorless solution was concentrated under vacuum to ca. 5 mL. Addition of *n*-hexane (10 mL) was added to precipitate complex **2** as a pale yellow solid. Yield: 0.162 g (87.3%). Anal. (%) Calcd for **2** ($C_{14}H_8$ $AuAg_2Cl_2F_9O_4S$): C 18.14, H 0.87, S 3.45. Found: C 17.99, H 0.93, S 3.29. ^1H NMR (75.5 MHz, $CDCl_3$, ppm): δ 3.42 (m, 4H, S−CH_2−CH_2−) and δ 2.21 (m, 4H, S−CH_2−CH_2−). ^{19}F NMR (282.4 MHz, $CDCl_3$, ppm): δ −89.8 (s, 2F, F_o), −115.92 (s, 1F, F_p) and −73.1 (s, 3F, $CF_3CO_2^-$). (MALDI-TOF −): *m*/*z* 997 ($[Au_2(C_6Cl_2F_3)_3]^-$, 27%), 865 ($[Ag_3(CF_3CO_2)_4(tht)]^-$, 13%), 597 ($[Au(C_6Cl_2F_3)_2]^-$, 100%). FT-IR (Nujol): $\nu(C_6Cl_2F_3)$ at 1586, 1556, 1061, and 771 cm^{-1}, ν(tht) at 1255 cm^{-1}, and $\nu(CF_3CO_2)$ at 1647 and 1204 cm^{-1}.

Synthesis of $[AuAg(C_6Cl_5)(CF_3CO_2)(tht)]_n$ (3). To a diethyl ether (20 mL) solution of $[Au(C_6Cl_5)(tht)]$ (0.107 g, 0.2 mmol) was added $[Ag(CF_3CO_2)]$ (0.044 g, 0.2 mmol). The solution turned pale yellow, and a solid started to precipitate. After 30 min of stirring the solution was concentrated under vacuum to ca. 5 mL. Addition of *n*-hexane (10 mL) led to precipitation of complex **3** as a white solid. Yield: 0.106 g (70.1%). Anal. (%) Calcd for **3** ($C_{12}H_8$ $AuAgCl_5F_3O_2S$): C 19.08, H 1.07, S 4.24. Found: C 19.06, H 0.91, S 3.81. ^1H NMR (75.5 MHz, $CDCl_3$, ppm): δ 3.20 (m, 4H, S−CH_2−CH_2−) and δ 2.20 (m, 4H, S−CH_2−CH_2−). ^{19}F NMR (282.4 MHz, $CDCl_3$, ppm): δ −73.0 (s, 3F, $CF_3CO_2^-$). (MALDI-TOF −): *m*/*z* 1140 ($[Au_2(C_6Cl_5)_3]^-$ 10%), 694 ($[Au(C_6Cl_5)_2]^-$ 100%). FT-IR (Nujol): $\nu(C_6Cl_5)$ at 843 and 628 cm^{-1}, ν(tht) at 1256 cm^{-1}, and $\nu(CF_3CO_2)$ at 1643 and 1202 cm^{-1}.

Crystallography. The crystals were mounted in inert oil on glass fibers and transferred to the cold gas stream of a Nonius Kappa (**1** and **2**) or a Bruker APEX2 (**3**) CCD area-detector diffractometer equipped with an Oxford Instruments low-temperature attachment. Data were collected by graphite-monochromated Mo Kα radiation ($\lambda = 0.71073$ Å). Scan type: ω and ϕ. Absorption corrections: numerical (based on multiple scans). The structures were solved by direct methods and refined on F^2 using the program SHELXL-97.[23] All non-hydrogen atoms were anisotropically refined (with the exception of the fluorine atoms of the disordered CF_3 groups in **1** and **2**), and hydrogen atoms were included using a riding model. Further details on the data collection and refinement methods can be found in Table 1. Selected bond lengths and angles are shown in Tables 2−4, and crystal structures of **1**−**3** can be seen in Figures 1−6. CCDC-652861−652863 contain the supplementary crystallographic data for this paper. These data can be obtained free of

(20) Fernández, E. J.; Laguna, A.; López-de-Luzuriaga, J. M.; Olmos, M. E.; Pérez, J. *Dalton Trans.* **2004**, 1801.

(21) Unpublished results

(22) (a) Usón, R.; Laguna, A.; Vicente, J. *J. Chem. Soc., Chem. Commun.* **1976**, 353. (b) Casado, A. L.; Espinet, P. *Organometallics* **1998**, *17*, 3677. (c) Usón, R.; Laguna, A.; Vicente, J.; García, J.; Bergareche, B. *J. Organomet. Chem.* **1979**, *173*, 349.

(23) Sheldrick, G. M. *SHELXL-97*; University of Göttingen: Göttingen, Germany, 1997.

charge via www.ccdc.cam.ac.uk/conts/retrieving.html (or from the Cambridge Crystallographic Data Centre, 12 Union Road, Cambridge CB2 1EZ, UK; fax: (+44) 1223-336-033; or e-mail: deposit@ccdc.cam.ac.uk).

Special Details. In complexes **1** and **2** one of the carbon atoms of a tht molecule (C(8) in **1** and C(9) in **2**) is disordered over two different positions (55:45). Both CF_3 groups in **1** and one of them in **2** are highly disordered, and the positions of their fluorine atoms have been modeled to a tetrahedral geometry and refined isotropically.

Computational Details. The model systems used in the theoretical studies of $[Au_2Ag_2(C_6F_5)_2(CF_3CO_2)_2(tht)_2]$ (**1a**) and $[AuAg_2R_2(CF_3CO_2)_2(tht)]$ ($R = C_6F_3Cl_2$ (**2a**) and C_6Cl_5 (**3a**)) were taken from the X-ray diffraction data for complexes **1**, **2**, and **3**, respectively. Keeping all distances, angles, and dihedral angles frozen, single-point DFT calculations were performed on model systems. In both the ground-state calculations and the subsequent calculations of the electronic excitation spectra, the B3LYP functional[24] as implemented in TURBOMOLE[25] was used. The excitation energies were obtained at the density functional level by using the time-dependent perturbation theory approach (TD-DFT),[26] which is a DFT generalization of the Hartree−Fock linear response (HF-LR) or random-phase approximation (RPA) method.[27] In all calculations, the Karlsruhe split-valence quality basis sets[28] augmented with polarization functions[29] were used (SVP). The Stuttgart effective core potential in TURBOMOLE was used for Au and Ag.[30]

Acknowledgment. This work was supported by the DGI-(MEC)/FEDER (CTQ2004-05495). R.C.P. thanks MEC for a grant.

Supporting Information Available: CIF files and TD-DFT results. This material can be obtained, free of charge, via the Internet at http://pubs.acs.org.

OM700701M

(24) (a) Becke, A. D. *J. Chem. Phys.* **1992**, *96*, 215. (b) Becke, A. D. *J. Chem. Phys.* **1993**, *98*, 5648. (c) Lee, C.; Yang, W.; Parr, R. G. *Phys. Rev. Lett. B* **1998**, *37*, 785.

(25) Ahlrichs, R.; Bär, M.; Häser, M.; Horn, H.; Kölmel, C. *Chem. Phys. Lett.* **1989**, *162*, 165.

(26) (a) Bauernschmitt, R.; Ahlrichs, R. *Chem. Phys. Lett.* **1996**, *256*, 454. (b) Bauernschmitt, R.; Ahlrichs, R. *J. Chem. Phys.* **1996**, *104*, 9047. (c) Bauernschmitt, R.; Häser, M.; Treutler, O.; Ahlrichs, R. *Chem. Phys. Lett.* **1997**, *264*, 573, and references therein. (d) Gross, E. K. U.; Kohn, W. *Adv. Quantum Chem.* **1990**, *21*, 255. (e) Casida, M. E. In *Recent Advances in Density Functional Methods, Vol. 1*; Chong, D. P., Ed,; World Scientific, 1995.

(27) Olsen, J.; Jørgensen, P. In *Modern Electronic Structure Theory, Vol. 2*; Yarkony, D. R., Ed.; World Scientific, 1995.

(28) Schäfer, A.; Horn, H.; Ahlrichs, R. *J. Chem. Phys.* **1992**, *97*, 2571.

(29) Dunning, T. H., Jr., *J. Chem. Phys.* **1994**, *100*, 5829.

(30) Andrae, D.; Haeussermann, U.; Dolg, M.; Stoll, H.; Preuss, H. *Theor. Chim. Acta* **1990**, *77*, 123.